Proceedings of the XVII ECSMGE-2019
Geotechnical Engineering foundation of the future
ISBN 978-9935-9436-1-3

doi: 10.32075/17ECSMGE-2019-0815

XVII European Conference
ECSMGE 2019
Reykjavik
on Soil Mechanics
and Geotechnical Engineering

Full dynamic analyses of embedded cantilever structures. A comparison between numerical analyses and simplified approaches

Analyse dynamique complète des paroi cantilever. Une comparaison entre les analyses numériques et les approches simplifiées

A. Oss
SWS Engineering SpA, Trento, Italy

F. Tabarelli, L. Simeoni
Department of Civil, Environmental and Mechanical Engineering, University of Trento, Italy

ABSTRACT: The design of earth retaining structures under seismic conditions is a challenging geotechnical problem. Simplified pseudo-static approaches are often adopted but they do not take into consideration the real performance of the structure during earthquake conditions. Italian building code (NTC) does not deal all aspects involved in the design. This paper shows a numerical study with Plaxis 2D through full dynamic analyses to analyze the soil-structure interaction. Three seismic signals and three different stiffness of the structures were adopted to investigate the behavior of a cantilever wall. Results from these numerical analyses in terms of earth pressure, displacements and stresses on the structures were compared to those obtained by the pseudo-static approaches.

RÉSUMÉ: La construction de structures de soutènement sous l'action du séisme est un problème géotechnique considérable. Ce problème est souvent traité à l'aide de solutions simplifiées, analyses pseudo-statiques par exemple. Cependant celles-ci sont loin de modéliser le comportement réel de la structure. La norme italienne pour les constructions (NTC) manque de précision et d'information sur ce sujet compliqué. Le document suivant propose une analyse numérique effectuée à l'aide du logiciel Plaxis2D pour mieux comprendre l'interaction terrain-structure par l'intermédiaire d'analyses dynamiques. Dans ce modèle, qui étudie le comportement sous séisme d'une paroi cantilever, nous avons considéré trois signaux sismiques et trois rigidités différentes de la structure. Les résultats en termes de pressions de sol, déplacements et contraintes dans la structure ont été comparés avec ceux du calcul pseudo-statique.

.

Keywords: cantilever retaining wall, earthquake, design

1 INTRODUCTION

The design of embedded cantilever retaining structures is usually based on simplified methods with approximate limit equilibrium calculations under static and seismic conditions. The most common approach is that proposed by Blum (1931), in which the wall is assumed to rotate rig-

idly around a pivot point located at a short distance from the wall tip (cantilever wall). The Blum's approach also assumed that a plastic mechanism occurs in the soil, and therefore the contact stresses are calculated as active (behind the wall) and passive (in front) earth pressures. In seismic conditions the pseudo-static method is often used by defining a seismic coefficient corresponding to a fraction of the maximum expected acceleration. The earthquake force is then replaced by a force with amplitude and direction constant with time. The force amplitude is defined by the seismic coefficient.

The design is aimed at defining the embedment depth, the internal forces in the retaining wall, as well as the permanent displacements produced by the earthquake.

Numerical analyses (Fourie et al., 1989, Callisto, 2014) have revealed that the distribution of the contact stresses is different from that proposed by the Blum's approach. Consequently, the internal forces based on the limit equilibrium methods may be greater or smaller than those obtained with the numerical analyses. In order to get a better accuracy of the limit equilibrium method, a different distribution of the contact stresses may be assumed (Conte et al., 2017).

The Italian building code (NTC 2018) admits the use of the simplified limit equilibrium approach for the design of embedded cantilevered or singly propped retaining walls, but do not give precise specifications on the distibution of the contact stresses.

This paper summarizes the results of fully-dynamic analyses carried out with the finite element code Plaxis2D (2017) for embedded cantilever walls with three different stiffness subjected to three different seismic inputs.

2 SIMPLIFIED DESIGN OF EARTH RETAINING STRUCTURES

The Specific European code for seismic design (EC8) and the Italian Building Code (NTC2008 recently updated with NTC2018) still allow the design of these structures using simplified methods, such as the pseudo-static approaches and the limited displacement design procedures.

2.1 Pseudo-static approaches

The Mononobe-Okabe solution (M-O) by Mononobe and Matsuo 1929, Okabe 1926, derives from the Müller-Breslau equation (1906) including the soil mass inertia forces. Therefore it adopts planar rupture surfaces, both for the active and the passive side. EC8 suggests the application of M-O equations in both sides, indeed it neglects the soil-wall friction in the passive side. When soil-wall friction needs to be considered other solutions may be assumed. For example, Lancellotta (2007) proposed a formulation based on the lower bound theorem of plasticity.

When active state is not reached, i.e. for high stiffness earth retaining walls subject to very low deformations, elastic conditions (referred to at-rest state of stress) are present before and during earthquake. Under these conditions, Wood (1973) has found a simple formulation to evaluate the thrust acting on a base-fixed wall. EC8 suggests the application of this formulation for structures that experience no deformations. Formulation was set-up for dry conditions so effects of drainage conditions can not be take into account. Further limits are the assumption of infinite stiffness of the structure. Recent works by Veletsos and Younan (1997), Younan and Veletsos (2000) have shown a significant reduction of pressures considering the wall flexibility.

2.2 Limited displacement methods

Newmark (1965) applied the acceleration time history to a sliding block analysis to estimate the relative displacement between a rigid body and a planar surface (Wotring and Andersen, 2001). Richard and Elms (1979) calculated the permanent displacements of a wall in terms of peak ground velocity (PGV) and peak ground acceleration (PGA). Further formulations to

calculate the permanent displacements were later proposed by Wong (1982), Whitman and Liao (1985). Rampello and Callisto (2008) developed a formulation through the integration of accelerograms recorded in Italy.

2.3 European and Italian codes

EC8 and NTC 2018 present some differences and limits about the seismic input to design earth retaining structures with the pseudo-static approaches. Differently to NTC2018, EC8 does not distinguish between rigid walls and embedded retaining structures. Both of them give the seismic coefficients as a fraction of the green-field PGA (a_g), corrected to take the soil type and the topographic local site effects into account, but with different formulations. EC8 expresses the horizontal seismic coefficicient k_h as:

$$k_h = \frac{a_g S \cdot S_T}{r} \quad (1)$$

where S and S_T are respectevely the soil type and the topography amplification factors, r is a factor depending on the wall deformation. Specifically, r ranges between 2 for walls that can accept displacements, to 1 in case of restrained displacement walls.

NTC2018 expresses k_h as:

$$k_h = \left(a_g S \cdot S_T\right) \cdot \alpha \cdot \beta \quad (2)$$

where α depends on the soil type and the wall total height while β depends on the maximum permanent displacement that the structure can tolerate.

Generally, vertical seismic coefficient k_v can be neglected. According to Whitman (1979), signal peaks having opposite sign result in a neglectable global effect during an earthquake.

Other differences between the stated codes are the way to express the seismic force:

- EC8 suggests to apply seismic force at the mid-height of the structure. M-O or Wood expressions are suggested as deformation state of the structure (active or at-rest state);
- NTC2018 doesn‘t give neither a formula to evaluate the seismic force nor the point of application for retaining structures. Indications are given only for rigid walls.

In this study, k_h was evaluated according to NTC2018.

3 NUMERICAL MODEL

Fully dynamic soil-structure interaction analyses were carried out in order to investigate the seismic performance of embedded cantilever retaining walls. The Finite Element commercial code PLAXIS (v. 2017) was used under 2D-plane strain conditions and by adopting a non-linear soil behaviour. Dry conditions were assumed and, therefore, the role of pore-water pressure was not investigated.

Analyses have considered three cantilever earth retaining structure with different stiffness and three different earthquake ground motions to analyze the dynamic response under different values of PGA and frequency content.

3.1 Acceleration time histories

Three different seismic signals were selected from the international databases: L‘Aquila earthquake (Italy) recorded on April 6, 2009 (ESMD), Emilia earthquake (Italy) recorded on May 20, 2012 (ESMD) and Tohoku-Sendai earthquake (Japan) recorded on March 11, 2011 (NIED). Main features of these acceleration histories are shown in Table 1.

Table 1. Main features of the acceleration histories

Earthquake	Code	PGA [g]	Moment magnitude	T [s]
L’Aquila	AQV	0.657	5.9	100
Emilia	MIRA	0.177	5.8	61
Tohoku-Sendai	HIT	1.209	9.0	300

In order to calibrate the Plaxis code, the recorded seismic inputs were compared to those obtained in free-field with Plaxis by applying the signals deconvoluted with the EERA code (Bardet et al., 2000), from the ground surface to the bedrock. A good agreement was generally found with only a little phase difference.

3.2 Soil profiles and parameters

A two-layers soil profile was considered: 4 m of sand above clay. Both soils were modeled with the Hardening Soil model with Small-strain Stiffness (HSsmall, Benz et al., 2009). The model allows to describe the hysteretic para-elastic soil behaviour at very small strain, by introducing the initial shear modulus G_o and the evolution of the secant shear stiffness ratio G_s/G_o with shear strain. Parameter $\gamma_{0.7}$ is the deformation at which the secant shear modulus is reduce to 70% of initial value G_0 and it defines the decay curve of shear modulus. Due to the lack of direct data, the shear modulus and damping ratio curves proposed by Seed and Sun (1989) for clays and by Seed and Idriss (1970) for sands were considered.

Soil parameters are shown in Table 2. Unit weight and Poisson's ratio are 19 kN/m^3 and 0.30 for sand, 20 kN/m^3 and 0.35 for clay.

3.3 Model description

Ground surface and soil layers are perfectly horizontal (Figure 1). The model is 30 m high and 150 m wide, with a ratio width/height equal to 5 to minimize the influence of the boundary conditions on the results.

Table 2. Soil parameters used in FEM analysis

Parameters	Sand	Clay
c' (kPa)	0	10
ϕ' (°)	35	25
m (-)	0.5	0.5
K_o (-) *	0.426	0.577
G_o (MPa) **	15.38	7.41
$\gamma_{0.7}$ (%)	0.02	0.07
E^{ref}_{50} (MPa)	8	4
E^{ref}_{ur} (MPa) ***	16	8
V_s (m/s)	89.13	60.28

* according to Jaky's expression for NC soils
** from $E_o = E_{50} \cdot 5$
*** $E_{ur} = E_{50} \cdot 2$

The mesh was composed by 13819 elements: in the central part for a width=50 m, where the wall is placed, the characteristic dimension h satisfies the condition proposed by Amorosi et al. 2008:

$$h \leq h_{max} = \frac{V_{s,min}}{(5 \div 10) f_{max}} \quad (3)$$

Where $V_{s,min}$ is the minimum value of the shear wave velocity and f_{max} is the maximum frequency of the seismic signal. For example, for $V_{s,min}$=60.28 m/s and f_{max}=10 Hz, h_{max} was assumed equal to 0.75 m.

To follow the construction process, the static stage was first simulated and then the dynamic phase was applied. Standard boundary conditions were assumed for the static stage. For the dynamic phase the seismic action was applied at the bottom of the model while lateral sides are set by adsorbent boundaries (Free field conditions).

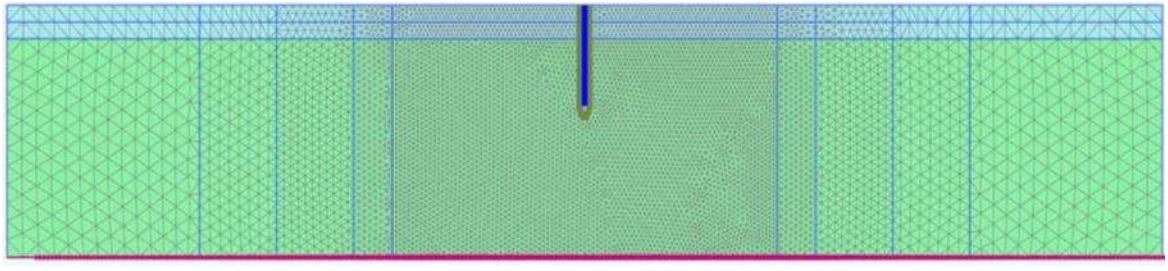

Figure 1. Numerical model for the dynamic analyses

Newmark method was set for the time integration under dynamic conditions. The Newmark's constants were set as α_N=0.3025 and β_N=0.600 that ensure the solution is unconditionally stable (Amorosi et al., 2012).

A Rayleigh damping of 5% was assumed for each layer and the corresponding Rayleigh coefficients α_R and β_R were assigned. The wall was simulated by Plate elements formulated according to the Mindlin theory. These elements are characterized by axial stiffness *EA* and flexural rigidity *EJ*, depending on the equivalent plate thickness. Interface elements were applied to simulate the soil-wall friction. A value of 0.7, typical to model a soil-concrete interaction, was considered.

3.4 Load cases

Cantilever walls with total length of 12 m and excavations with depth of 4 m were simulated. To investigate the effects of the structure stiffness, three different wall thickness were considered: 0.79 m, 0.58 m and 0.37 m.

The seismic input (AQV, MIRA, HIT) were applied at the bottom of the numerical model (height=30 m) through a preliminary deconvolution process with EERA. Considering that each wall was subject to three seismic input, a total of nine different cases were simulated.

4 RESULTS

4.1 Earth pressure distribution

Figure 2, 3 and 4 show the horizontal pressure distributions after the excavation (static) and at the end of the seismic shaking (dynamic). Static and dynamic results are compared, respectively, to the pressure distibutions obtained with the Müller-Breslau (MB) and M-O solutions, for the active state, with the Lancellotta solution (LAN), for the passive state.

Table 3. Ratios $S_{h,dyn}/S_{h,stat}$ *for different wall stiffness (behind the wall)*

Earthquake	B_{eq}=0.79m	B_{eq}=0.58m	B_{eq}=0.37m
AQV	1.23	1.25	1.25
MIRA	1.14	1.14	1.14
HIT	1.82	1.77	1.77

Table 4. Ratio between $S_{h,dyn}/S_{h,stat}$ *for different wall stiffness (in front of the wall)*

Earthquake	B_{eq}=0.79m	B_{eq}=0.58m	B_{eq}=0.37m
AQV	1.24	1.25	1.25
MIRA	1.14	1.15	1.14
HIT	1.83	1.77	1.79

4.1.1 Behind the wall

For the AQV input, the ¨dynamic¨ pressures at the end of the seismic motion exceed the static ones up to 2 meters below the excavation level. The ¨dynamic¨ pressure distribution shows a good agreement with M-O. For the MIRA input, the ¨dynamic¨ pressures follow the static trend along all the wall length. For the HIT input, the ¨dynamic¨ pressures exceed the static trend, but remains quite constant from the middle of the excavation depth to its bottom. In this case, the M-O solution underestimates the pressures.

It is interesting to evaluate the ratio $S_{h,dyn}/S_{h,stat}$ between the dynamic and static resulting forces as a function of the wall stiffness. Table 3 shows that this ratio depends on the seismic input but it is quite indipendent from the stiffness.

4.1.2 In front of the wall

Compared to the static pressure distribution, where the passive resistance is reached only near the excavation level, the dynamic pressure distibutions are generally higher. For AQV and MIRA seismic input, the dynamic pressure distributions are significantly less than the LAN solution. In the case of the HIT input, the dynamic pressures equals the LAN solution for nearly 1 m below the excavation level.

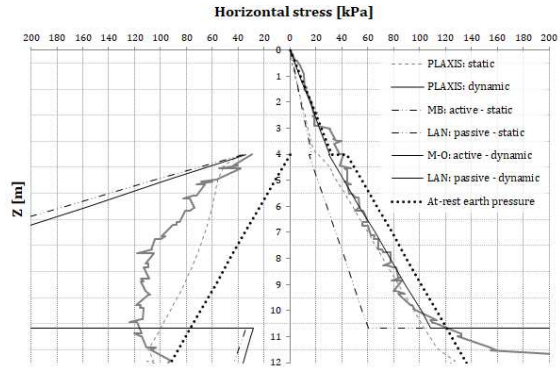

a)

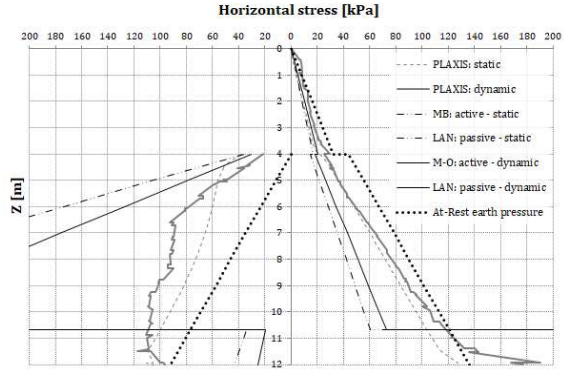

b)

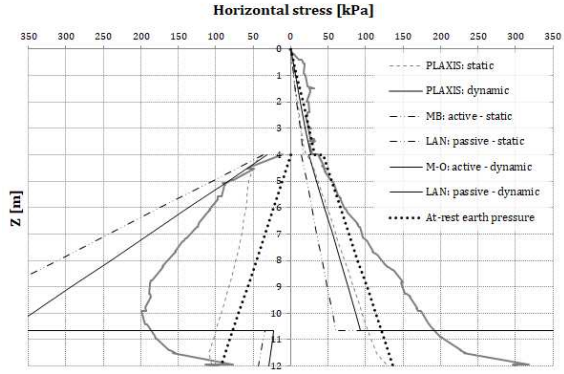

c)

Figure 2. Horizontal stress distribution (B_{eq}=0.79 m) for three seismic inputs: a) AQV; b) MIRA; c) HIT

Considerations on the ratio $S_{h,dyn}/S_{h,stat}$ are similar to those for the side behind the wall (Table 4). It is interesting to note that the ratios

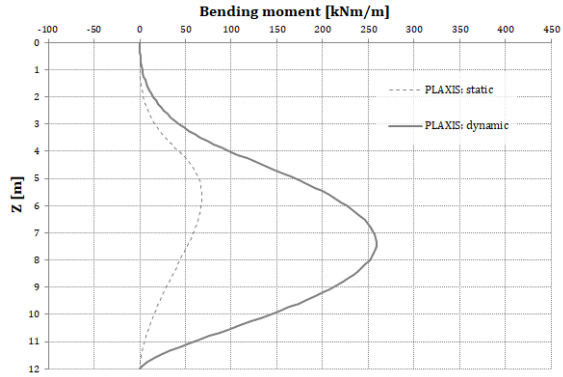

Figure 3. Bending moment distribution for AQV input (B_{eq}=0.79 m)

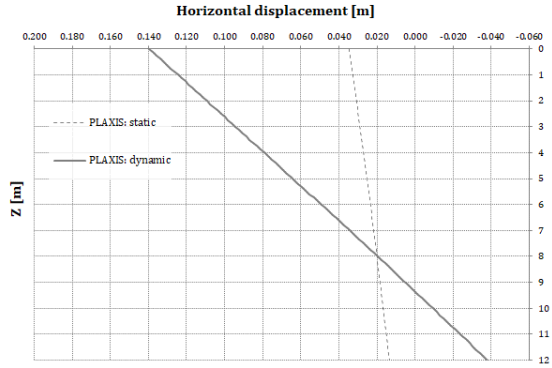

Figure 4. Horizontal displacement distribution for AQV input (B_{eq}=0.79 m)

have very similar values in both sides of the walls.

4.2 Stresses on the wall

Figure 3 compares the dynamic and static bending moments for the AQV seismic input. For all the case studies, general comments can be done:

- The increase due to the earthquake resulted well noticeable;
- The position of the maximum bending moment always differed from that of the static one. In general, the maximum bending moment occurred at the position of 0.63 times the wall total length.

Table 5. Dynamic and static maximum bending moment ratios for different wall stiffnesses

Signal	B_{eq}=0.79m	B_{eq}=0.58m	B_{eq}=0.37m
AQV	3.80	3.85	3.70
MIRA	2.56	2.54	2.60
HIT	4.85	4.65	4.98

Table 6. Dynamic and static maximum shear force ratios for different wall stiffness

Signal	B_{eq}=0.79m	B_{eq}=0.58m	B_{eq}=0.37m
AQV	5.49	5.45	5.09
MIRA	3.17	3.25	3.26
HIT	6.97	6.94	7.46

Table 7. Comparison between permanent displacements from numerical analyses and simplified methods

Signal	B_{eq}=0.79m	Newmark [m]	Rampello-Callisto [m]
AQV	0.140	0.251	0.339
MIRA	0.072	0.030	0.012
HIT	231.0 *	0.410	0.199

* large value, cause is currently investigated

Table 5 summarizes the ratio between dynamic and static bending moments. Results show low dependency of stiffness. Similar results are obtained for the shear forces (Table 6).

4.3 Displacements

Figure 4 shows the trend of displacements referred to the AQV input. Diplacements are calculated at the end of the seismic input, so they are permanent displacements. A comparison is performed to the simplified methods in Table 7. The Newmark and Rampello-Callisto simplified methods were considered. These methods do not take the wall stiffness into account so the comparison is limited only to the case B_{eq}=0.79 m. It is shown that simplified methods predicted reasonable values only for the MIRA input while for the other inputs results are quite different from the dynamic analyses. The application of the Newmark method (founded on rigid block analysis) to earth retaining walls is characterized by some incertaines (Callisto and Aversa, 2008). Main ambiguities are related to associate the rigid block theory to the rotational kinematisms observed with the numerical analyses for the cantilever walls.

5 CONCLUSIONS

Differences between full dynamic analyses and pseudo-static approaches resulted in terms of pressure distribution and displacements in a way depending on the seismic input.

6 REFERENCES

Amorosi, A., Boldini, D., Sasso, M. 2008. Modellazione numerica del comportamento dinamico di gallerie superficiali in terreni argillosi, *Rapporto di ricerca*, University of Bologna, Italy.

Amorosi, A., Boldini, D., Postiglione, G. 2012. Analysis of tunnel behaviour under seismic loads: the role of soil constitutive assumptions, *Second International Conference on Performance-based Design in Earthquake Geotechnical Engineering*, Taormina, Italy.

Bardet, J.P., Ichii, K., Lin, C.H. 2000. EERA-A computer program for Equivalent-linear Earthquake site Response Analyses of layered soils deposits, *Computer and Geotechnics* **37**, 515-528.

Benz, T., Vermeer, P.A., Schwab, R. 2009. A small strain overlay model, *International Journal for Numerical and Analytical Methods in Geomechanics* **33**, 25-44.

Blum, H. 1931. Einspannungsverha¨ltnisse bei Bohlkwerken. *Wil. Ernst und Sohn* (in German), Berlin, Germany.

Callisto, L. 2014. Capacity design of embedded retaining structures. *Géotechnique* 64, 3, 204–214.

Callisto, L., Aversa, S. 2008. Dimensionamento di opere di sostegno soggette ad azioni sismiche, *Proceedings of MIR 2008*, Pàtron Editore, Bologna, IT.

Conte, E., Troncone, A., Vena, M. 2017. A method for the design of embedded cantilever retaining walls under static and seismic loading, *Géotechnique* 67, 12, 1081–1089.

De Luca, F., Chioccarelli, E., Iervolino, I. 2011. Preliminary study of the 2011 Japan earthquake (M 9.0) ground motion records V1.01, *available at http://www.reluis.it.*

ESMD (European Strong Motion Database).

Fourie, A. B. & Potts, D. M. 1989. Comparison of finite element and limiting equilibrium analyses for an embedded cantilever retaining wall. *Géotechnique* 39, No. 2, 175–188.

Lancellotta, R. 2007. Lower-bound approach for seismic passive earth resistance, *Géotechnique* **57**, 3, 319-321.

Ministero delle Infrastrutture e dei Trasporti. 2013. Rapporto di analisi di risposta sismica locale per la ricostruzione del Palazzo del Governo della citta dell'Aquila, *available at http://www.mit.gov.it/mit/mop_all.php?p_id=15722.*

Mononobe, N., Matsuo, H. 1929. On the determination of earth oressures during eartquakes, *Proceedings World Engineering Congress* **9**, 275.

Müller-Breslau, H. 1906. Erddruck auf Stuetzmauern, *Kroener*, Stuttgart.

Newmark, N.M. 1965. Effects of earthquakes on dams and embankments, 5th Rankine lecture, *Géotechnique* **15 (2)**, 139-193.

NIED (National Research Institute for Earth Science and Disaster Resilience).

Okabe, S. 1926. General theory of earth pressures, *Journal Japan Soc. Eng.* **12 (I)**, Tokyo.

Plaxis Bv. 2017. User's Manual.

Rampello, S., Callisto, L. 2008. Stabilità dei pendii in condizioni sismiche, *Proceedings of MIR 2008*, Pàtron Editore, Bologna, IT.

Regione Emilia-Romagna. 2015. Relazione geologica-geotecnica per il progetto e realizzazione di 2 edifici scolastici - Adeguamento dell'est esistente e riqualificazione urbana dei relativi collegamenti ciclo-pedonali.

Richard, R., Elms, D.G. 1979. Seismic behavior of gravity retaining walls, *Journal of the Geotechnical Engineering Division*, ASCE **105**, 449-464.

Seed, H.B., Idriss, I.M. 1970. Soil Moduli and damping factors for dynamic response analysis, *EERC-Report 70-10*, Berkeley, CA.

Seed, H.B., Sun, J.H. 1989. Implication of site effects in the Mexico City earthquake of September 19, 1985 for Earthquake-Resistant Design Criteria in the San Francisco Bay Area of California, *Report No. UCB/EERC-89/03*, Earthquake Engineering Research Center, University of California, Berkeley, CA.

Veletsos, A.S., Younan, A.H. 1997. Dynamic response of cantilever retaining walls, *Journal of Geotechnical and Geoenvironmental Engineering*, ASCE, **123 (2)**, 161-172.

Whitman, R.V. 1979. Dynamic behavior of soils and its application to civil engineering projects, State of the Art Report, *6th Pan. Conf. SMFE* **1-59**, 105, Lima.

Whitman, R.V., Liao, S. 1985. Seismic design of gravity retaining walls, *Proceedings 8th World Conf. On Earth Engineering* **3**, 533-540, San Francisco, CA.

Wong, C.P. 1982. Seismic analysis and improved seismic design procedure for gravity retaining walls, *MSc Thesis*, Department of Civil Engineering, MIT, Cambridge, MA.

Wood, J.H. 1973. Earthquake-induced soil pressure on structures, *PhD thesis*, California Institute of Technology, Pasadena, CA.

Wotring, D., Andersen, G. 2001. Displacement-Based Design Criteria for Gravity Retaining Walls in Light of Recent Earthquakes, *International Conferences on Recent Advances in Geotechnical Earthquake Engineering and Soil Dynamics* **20**.

Younan, A.H., Veletsos A.S. 2000. Dynamic response of flexible retaining walls, *Earthquake Engineering and Structural Dynamics* **29**, 1815-1844.